doi:10.1016/j.jmb.2004.02.069 J. Mol. Biol. (2004) 338, 217–228

JMB

Available online at www.sciencedirect.com

SCIENCE DIRECT®

ELSEVIER

Structural and Functional Characterization of Mitochondrial EndoG, a Sugar Non-specific Nuclease which Plays an Important Role During Apoptosis

Patrick Schäfer[1]†, Sebastian R. Scholz[1]†, Oleg Gimadutdinow[2] Iwona A. Cymerman[3], Janusz M. Bujnicki[3], Adolf Ruiz-Carrillo[4] Alfred Pingoud[1] and Gregor Meiss[1]*

[1]*Institute of Biochemistry Justus-Liebig-University Heinrich-Buff-Ring 58 D-35392 Giessen, Germany*

[2]*Department of Genetics Kazan State University Kremlevskaja 18, 420008 Kazan, Russian Federation*

[3]*Bioinformatics Laboratory International Institute of Molecular and Cell Biology Trojdena 4, 02-109 Warsaw Poland*

[4]*Department of Molecular and Cell Biology, Institute of Molecular Biology of Barcelona (IBMB), CID-CSIC Jordi Girona 18-26 08034 Barcelona, Spain*

**Corresponding author*

Combining sequence analysis, structure prediction, and site-directed mutagenesis, we have investigated the mechanism of catalysis and substrate binding by the apoptotic mitochondrial nuclease EndoG, which belongs to the large family of DNA/RNA non-specific ββα-Me-finger nucleases. Catalysis of phosphodiester bond cleavage involves several highly conserved amino acid residues, namely His143, Asn174, and Glu182 required for water activation and metal ion binding, as well as Arg141 required for proper substrate binding and positioning, respectively. These results indicate that EndoG basically follows a similar mechanism as the *Serratia* nuclease, the best studied representative of the family of DNA/RNA non-specific nucleases, but that differences are observed for transition state stabilisation. In addition, we have identified two putative DNA/RNA binding residues of bovine EndoG, Arg135 and Arg186, strictly conserved only among mammalian members of the nuclease family, suggesting a similar mode of binding to single and double-stranded nucleic acid substrates by these enzymes. Finally, we demonstrate by ectopic expression of active and inactive variants of bovine EndoG in HeLa and CV1-cells that extramitochondrial active EndoG by itself induces cell death, whereas expression of an enzymatically inactive variant does not.

Keywords: apoptosis; nuclease; endonuclease G; active-site; catalysis

Introduction

The mitochondrial endonuclease G (EndoG) is an enzyme involved in a variety of cellular functions, ranging from the generation of primers for mitochondrial DNA replication to the initiation of genomic inversion in herpes simplex type-1 virus (HSV-1).[1–3] One of the most recent findings is, that upon apoptotic stimuli, EndoG can be released from mitochondria and then contributes to the degradation of chromosomal DNA during apoptosis.[4–6] Database searches reveal that EndoG is a member of an ancient family of DNA/RNA non-specific nucleases. Nucleases of this family are found in a large number of pro- and eukaryotic organisms, including bacteria, protozoa, fungi and slime moulds, invertebrates and vertebrates.[7] The prokaryotic nucleases are usually secreted by their bacterial hosts and are likely to serve nutritional purposes, whereas in eukaryotic organisms these nucleases are targeted to mitochondria and, e.g. in *Caenorhabditis elegans* and mammals, contribute to apoptotic DNA degradation.[4,5,8,9] One of the structurally and mechanistically best characterized members of the DNA/RNA non-specific nucleases is the extracellular nuclease of *Serratia marcescens*.[10–12]

Mammalian EndoG is encoded in the nucleus and produced as a ~33 kDa preprotein with a mitochondrial targeting sequence at its N

† P.S. and S.R.S. contributed equally to this work.

Abbreviations used: EndoG, mitochondrial endonuclease G; HSV-1, herpes simplex type-1 virus; AIF, apoptosis inducing factor; tEndoG, truncated bovine EndoG; WAH-1, worm-AIF-homolog 1.

E-mail address of the corresponding author: gregor.meiss@chemie.bio.uni-giessen.de

terminus.[13] Upon translocation into mitochondria, the targeting sequence is cleaved off to give rise to the ~28 kDa mature nuclease.[2] Degradation of nucleic acids by the mature nuclease is prevented in healthy cells through the compartmentalisation of EndoG in the mitochondrial intermembrane space.[14] After induction of apoptosis, mitochondria release the nuclease together with other mitochondrial proteins, such as cytochrome *c* and apoptosis

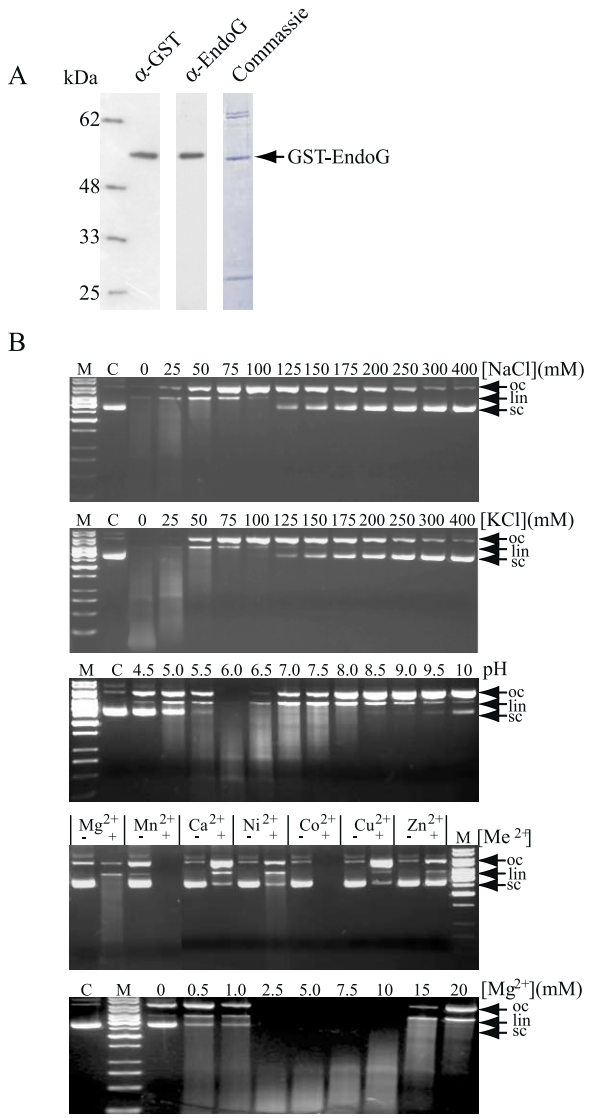

Figure 1. Properties of recombinant EndoG overexpressed and purified from HEK-293T-cells. A, Transfection-mediated overexpression and purification of GST-tEndoG was analyzed by immunoblotting using anti-GST (α-GST) and anti-EndoG (α-EndoG) antibodies as well as by Coomassie staining of an SDS-polyacrylamide gel. B, The pH profile of GST-tEndoG was analysed as described in Materials and Methods. The enzyme is most active at pH 6.0. At higher pH values it has the tendency to nick the DNA substrate rather than introducing double-strand breaks as judged by the accumulation of the open circular form of plasmid DNA. It is able to use a variety of divalent metal ion cations as a cofactor. For Mg^{2+}, the concentration optimum is around 2.5–5.0 mM.

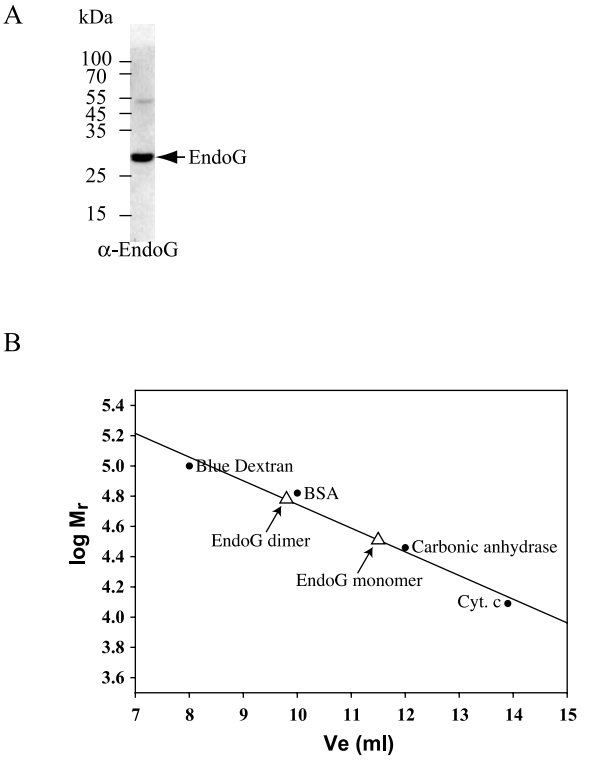

Figure 2. Gel-filtration analysis of the quaternary structure of EndoG. A, GST-tEndoG was treated with thrombin overnight and proteolytic processing monitored by immunobloting using an anti-EndoG antibody. B, Thrombin-treated EndoG was chromatographed subsequently over a Superdex 75 HR 10/30 column, which results in two active fractions eluting at the size of BSA and carbonic anhydrase, corresponding to the monomer and dimer of EndoG (white triangles), respectively. Standard proteins are indicated by black dots.

inducing factor (AIF), enabling EndoG to degrade chromosomal DNA.[4,5] In contrast to the caspase-activated DNase (CAD/DFF40), it has been reported that mammalian EndoG can be activated in a caspase-independent manner, triggered by the release of the pro-apoptotic factor Bim from microtubuli.[4] It has been shown that the *C. elegans* EndoG-ortholog CPS-6 interacts with the worm-AIF-homolog 1 (WAH-1), suggesting a common role of WAH-1/AIF and CPS-6/EndoG in nuclear apoptotic changes such as chromatin condensation as well as large-scale and nucleosomal DNA fragmentation.[15] In *C. elegans*, six additional so-called "cell-death-related nucleases" have been identified that cooperate with CPS-6/EndoG and thus contribute to apoptotic DNA degradation.[9]

Here, we present a detailed structural and functional characterisation of bovine EndoG. Homology modelling and site-directed mutagenesis experiments suggest that the enzyme has a similar structure and exhibits a similar mechanism of action as the related nuclease from *S. marcescens*. Furthermore we show that ectopic expression of enzymatically active extramitochondrial EndoG induces cell death, suggesting

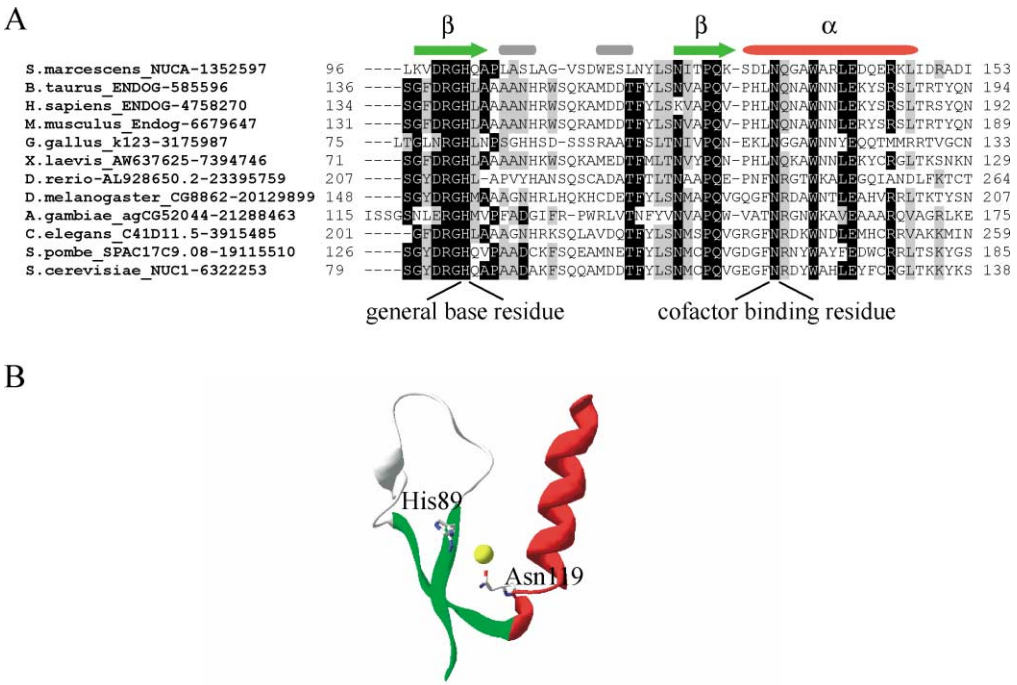

Figure 3. EndoG is a DNA/RNA non-specific nuclease belonging to the superfamily of ββα-Me-finger nucleases. A, Sequence comparison of the active-site region of selected DNA/RNA non-specific nucleases. The DRGH-motif contains several catalytically important amino acid residues, in particular the general base histidine. The highly conserved asparagine residue in *Serratia* nuclease is the sole direct cofactor ligand, essential for divalent metal ion binding. B, The active-site of *Serratia* nuclease shows the typical ββα-Me-finger fold that is also found in a variety of other nucleases (see the text).

that, in principle, EndoG could be used to trigger cell killing.

Results and Discussion

Biochemical properties of recombinant bovine EndoG

In order to perform a biochemical analysis of EndoG, we have established a system for transfection-mediated overexpression of a GST-fusion protein of mature bovine EndoG in HEK 293-T cells. The purified GST fusion protein shows the expected size when analysed by SDS-PAGE and immunoblotting using anti-GST and anti-EndoG antibodies (Figure 1). The biochemical properties of the fusion protein are identical with those reported for recombinant human EndoG produced using a baculoviral system,[16] with the exception of the pH profile for optimum activity (Figure 1B). In contrast to a biphasic pH-profile reported earlier,[16] we have found a monophasic pH-profile with an optimum around pH 6. Since apoptotic cells show cytosolic acidification,[17] the pH optimum of EndoG might reflect an adaptation of the enzyme to low pH, emphasizing its role as an apoptotic nuclease (Figure 1B). GST-tEndoG is most active at low-salt conditions, and, like other DNA/RNA-non-specific nucleases, accepts a variety of divalent metal ions as a cofactor ($Co^{2+} > Mn^{2+} > Mg^{2+} \approx Ni^{2+} > Ca^{2+} > Zn^{2+}$). The concentration optimum for Mg^{2+} is rather broad with a peak around 2.5–5.0 mM.

EndoG exhibits a monomer/dimer-equilibrium

Earlier studies with EndoG purified from calf thymus nuclei and whole tissue demonstrated that in gel-filtration experiments the native enzyme behaves like a dimer with an apparent molecular mass of 50 kDa.[18] Treatment of GST-tEndoG expressed in 293T-HEK cells with thrombin resulted in the complete cleavage of the fusion protein and release of the nuclease (Figure 2). When this protein preparation was subjected to gel-filtration over a Superdex-75 column, nucleolytic activity was found in two well-separated fractions obtained at positions corresponding to a dimeric and monomeric enzyme, respectively (Figure 2), extending the previous observations, and indicating that under the conditions applied EndoG exists in a monomer–dimer equilibrium. It had been shown previously that the related *Serratia* nuclease (see below), a homodimer in the crystal,[19] also exists in a monomer–dimer equilibrium, with the active sites acting independently from each other.[20] It is noteworthy that engineered obligatory monomeric variants of the *Serratia* nuclease are fully active.[20]

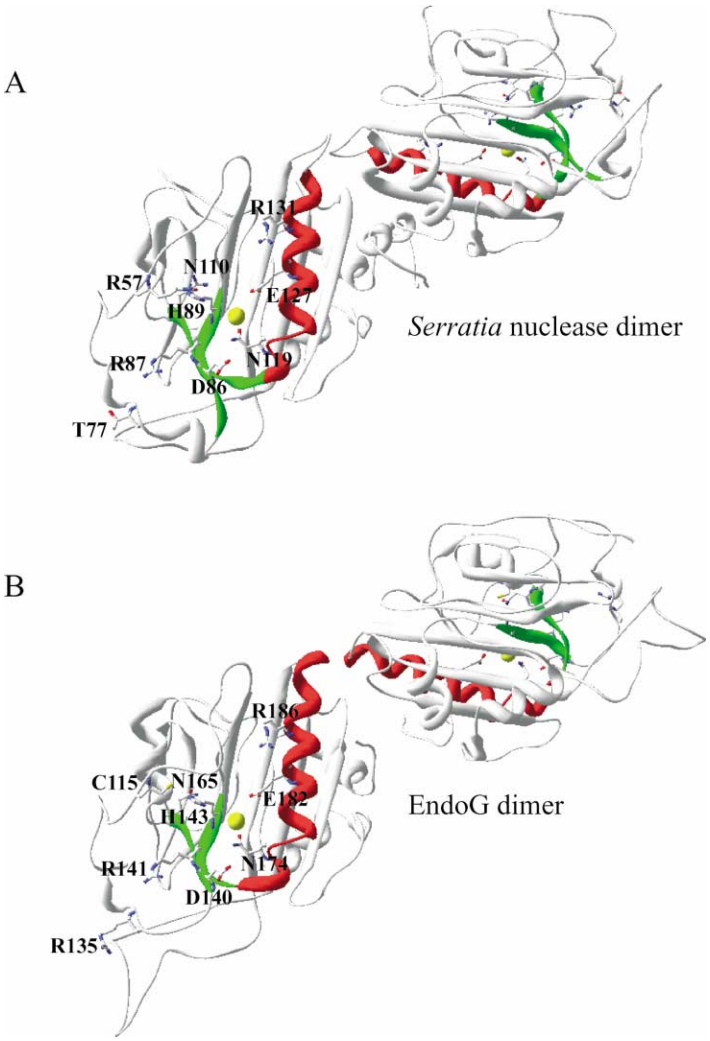

Figure 4. Structural model of EndoG in comparison with the *Serratia* nuclease structure. A, *Serratia* nuclease dimer with the ββα-Me-finger motif highlighted in green (β-sheets) and red (α-helices). Also shown are the residues Arg57, Thr77, Asp86, Arg87, His89, Asn110, Asn119, Glu127 and Arg131 (corresponding to Cys115, Arg135, Asp140, Arg141, His143, Asn165, Asn174, Glu182 and Arg186 of EndoG) as well as the divalent metal ion cofactor in the catalytic centre of this nuclease.

EndoG belongs to the family of DNA/RNA non-specific nucleases

A primary sequence analysis demonstrates that EndoG belongs to the large family of DNA/RNA-non-specific nucleases (Figure 3A). The active site of these nucleases is characterised by the DRGH-motif, which contains the catalytically important histidine residue and structurally is part of the ββα-Me-finger motif (Figure 3B). The ββα-Me-finger is found in many nucleases that exhibit globally distinct structures, including the structure specific phage T4 endonuclease VII,[21] the DNase colicins.[22–24] and homing endonucleases of the H-N-H-family and His-Cys box-family.[25–27] Intriguingly, recent findings suggest that the caspase-activated DNases also belong to this superfamily.[28,29] In the family of DNA/RNA non-specific nucleases the *Serratia* nuclease has been studied extensively in terms of structure and catalytic mechanism.[10–12]

Homology modelling of bovine EndoG

We have generated a homology model of the three-dimensional structure of bovine EndoG, using the crystal structure of the *Serratia* nuclease[30] as a template (Figure 4). A comparison of the *Serratia* nuclease structure with the EndoG model† reveals that nearly all residues known to be critical for the activity of the *Serratia* enzyme are present in EndoG, with two exceptions: (i) a cysteine residue (Cys115) in bovine EndoG is found at a position corresponding to Arg57 of *Serratia* nuclease, which there is thought to be required for transition state stabilisation in the catalytic mechanism of this enzyme[12]; and (ii) an arginine residue is found at position 135 in bovine EndoG that corresponds to Thr77 in *Serratia* nuclease (Figure 4).

Catalytic mechanism of EndoG

The structural model and the sequence alignment of EndoG with DNA/RNA-non-specific nucleases provide a rationale for site-directed mutagenesis to identify important active-site residues. DNA cleavage kinetics with several

† ftp://genesilico.pl/iamb/models/endoG

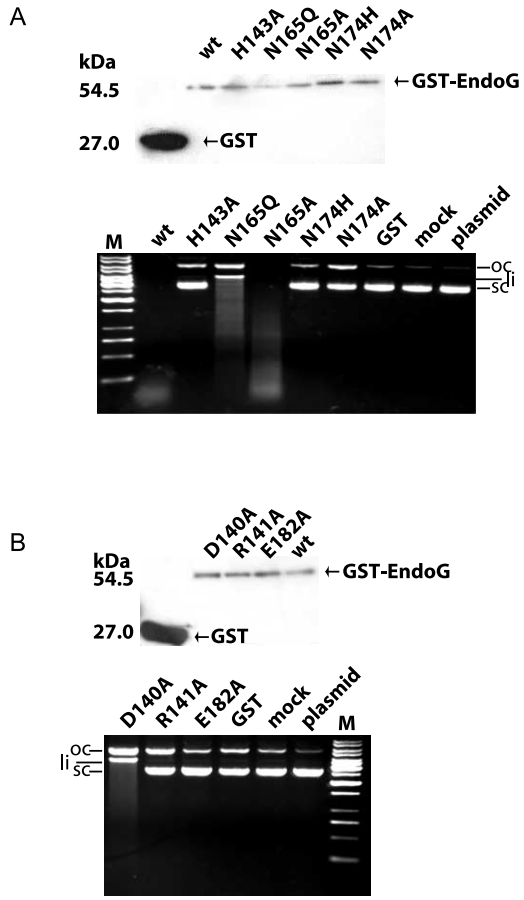

Figure 5. Mutagenic scan of catalytically relevant amino acid residues of EndoG. All EndoG mutants were overexpressed as GST-fusion proteins in HEK 293-T cells and purified over glutathione Sepharose-4B beads. Expression was monitored by blotting using an anti-GST antibody. Nucleolytic activity was measured by cleavage of plasmid DNA by EndoG variants. Mock transfected cell extracts and GST expressed and purified in parallel were used for control experiments. A, Catalytically relevant residues conserved in the superfamily of ββα-Me-finger nucleases. The histidine residue (His134 in bovine EndoG) is required for water activation, while the asparagine residue (Asn174 in bovine EndoG) is responsible for cofactor binding. B, Catalytically relevant residues conserved in the family of DNA/RNA non-specific nucleases. Asp140 and Arg141 are part of the DRGH-motif of these nucleases. Glu182 is most likely involved in metal ion binding, as is Glu127 in the *Serratia* nuclease.

Table 1. Properties of bovine EndoG variants with substitution of conserved amino acid residues

Position	Substitution	Rel. activity (%)[a]	Putative function
Wild-type	–	100	
Cys115	Ala	84	No major catalytic function
	Arg	17	
	Ser	91	
Arg135	Ala	49	DNA binding
	Lys	34	
Asp140	Ala	46	Active-site conformation
Arg141	Ala	n.d.c.	DNA binding and positioning
His143	Ala	n.d.c.	Water activation
Asn165	Ala	46	Active-site conformation
	Gln	46	
Asn174	Ala	<1	Cofactor binding
	His	4	
Glu182	Ala	n.d.c.	Cofactor binding *via* water
Arg186	Ala	11	DNA binding
	Lys	6	

n.d.c.—no detectable cleavage.
[a] The nucleolytic activity, determined in cleavage assays with supercoiled plasmid DNA, was normalized to the same amount of immunoreactive material.

variants carrying amino acid exchanges at critical positions suggested by the EndoG model and the sequence alignment of DNA/RNA non-specific nucleases, identify the amino acid residues Asp140, Arg141 and His143 from the DRGH-motif of bovine EndoG as being important for activity (Figure 5 and Table 1). Substitution of the conserved amino acid residues Asn174 and Glu182 by alanine, also leads to inactive enzyme variants (Figure 5 and Table 1). In contrast, exchange of Cys115 to alanine, serine or arginine, respectively, does not lead to a dramatic loss in enzymatic activity (a factor of 2 in the case of the C115R variant), suggesting that this amino acid residue does not play a major role in the catalytic mechanism of bovine EndoG, although it is at a position corresponding to Arg57 of *Serratia* nuclease, which is supposed to be required for transition state stabilisation by neutralising the extra negative charge of the transition state (Figure 5 and Table 1).[12] At best, Cys115 could form a hydrogen bond to one of the non-bridging oxygen atoms of the phosphodiester group. Similarly, Asn165 of bovine EndoG, when substituted by alanine or glutamine does not lead to a severe loss of enzymatic activity, although this residue is at a position corresponding to the structurally important asparagine residue of H-N-H enzymes, such as colicin E9 and E7,[23,31] which also belong to the family of ββα-Me-finger nucleases.

On the basis of our experimental results it seems very likely that EndoG follows a mechanism that is similar, in part, to that of the *Serratia* nuclease. We suggest that His143 of bovine EndoG activates a water molecule, generating a nucleophile that attacks the scissile phosphodiester bond (Figure 6), similar to His89 of Serratia nuclease.[11,12] The *Serratia* nuclease contains a unique Mg^{2+}–water cluster at the active site in which Asn119 is the only direct metal ion ligand, whereas all other positions of the octahedrally bound metal ion are contacted indirectly *via* water molecules, as deduced from the crystal structure.[32] In the case of bovine EndoG we assume that Asn174 takes over

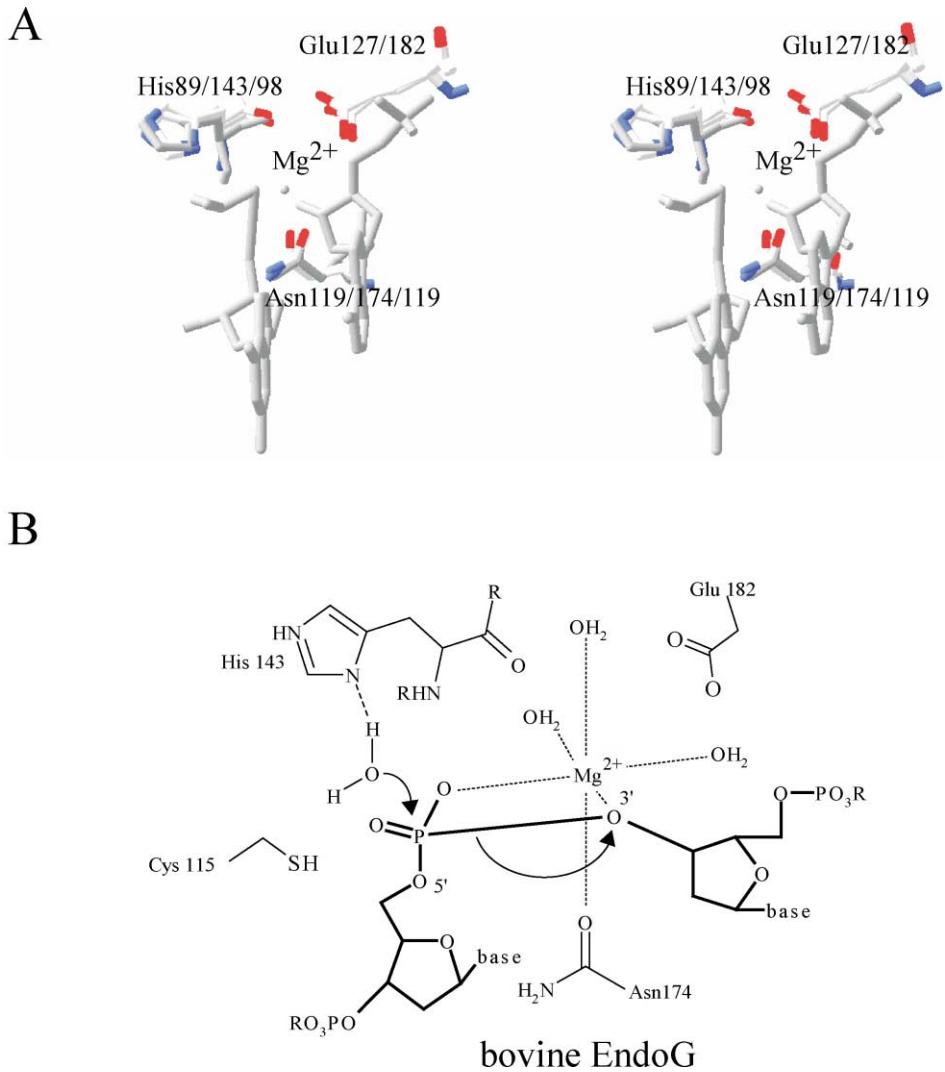

Figure 6. Catalytic centre and mechanism of phosphodiester bond cleavage by EndoG. A, Stereo representation of the active-site residues of the model of EndoG (His143, Asn174, and Glu182) and *Serratia* nuclease (His89, Asn119, and Glu127) superimposed with those of the I-*Ppo*I (His98 and Asn119) in complex with product DNA (1ipp). B, Proposed catalytic mechanism of EndoG: His143 of EndoG activates a water molecule generating a hydroxide ion that attacks the scissile phosphodiester bond, as does His89 of *Serratia* nuclease. Like in the *Serratia* nuclease structure (1qae) the obligatory divalent metal ion cofactor is coordinated by five solvent water molecules and an asparagine residue (Asn119 in *Serratia* nuclease, Asn174 in EndoG) as the sole direct protein ligand. In the catalytic mechanism, two of the water molecules from the coordination sphere of the metal ion upon DNA binding are replaced by oxygen atoms from the phosphodiester moiety. As proposed for *Serratia* nuclease, in which a water molecule from the hydration sphere of the divalent metal ion cofactor serves to protonate the leaving group, leaving group protonation in EndoG could be achieved in the same way. How EndoG stabilises the transition state is not clear from our study. In principle, this function could be taken over by the divalent metal ion cofactor, with a minor contribution from Cys115 due to its capacity to form a hydrogen bond to the negatively charged non-bridging P–O oxygen.

the role of the direct metal ion ligand (Figure 6). Different from *Serratia* nuclease, in which Arg57 serves to neutralise the extra negative charge developing during the transition state, there is no obvious amino acid residue located at the active site of EndoG that could stabilise the transition state. Instead, a cysteine residue (Cys115) is found at the corresponding position in EndoG which is not very well suited for such a function. Indeed, our results indicate that Cys115 is not of major importance for catalysis. As there is no good candidate for an amino acid residue to have this function for EndoG, we suggest that the divalent metal ion cofactor is involved in transition state stabilisation.

Several arginine residues contribute to the binding of nucleic acids by EndoG

In the modelled structure of EndoG, two arginine residues, Arg135 and Arg186, are arranged "in line" with Arg141 and His143, suggesting that these residues, which are more distant from the presumptive catalytic centre, may be involved in

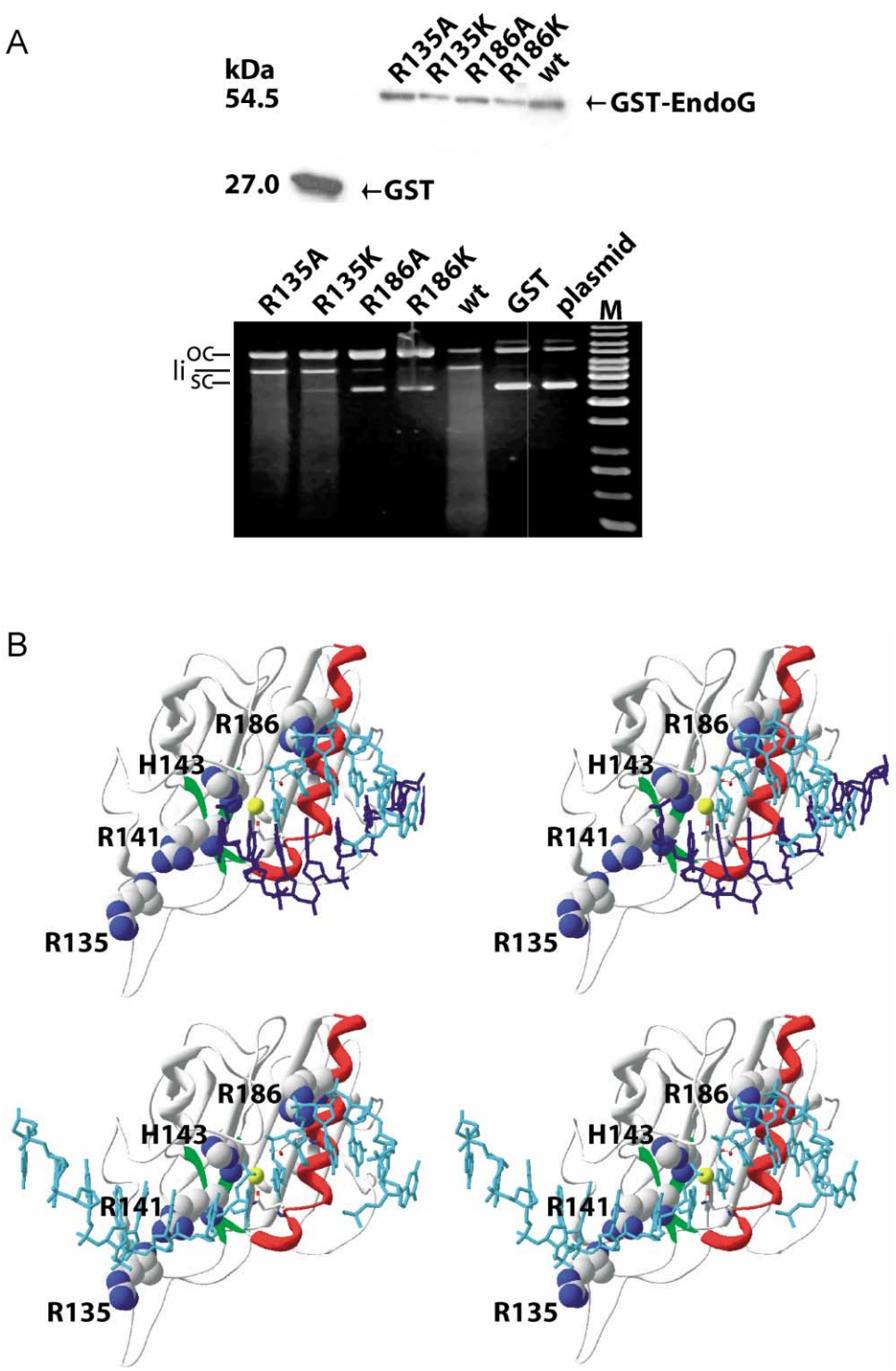

Figure 7. DNA binding by EndoG. A, Mutagenic scan of putative DNA-binding amino acid residues of EndoG. All EndoG mutants were overexpressed as GST-fusion proteins in HEK 293-T cells and purified over glutathione Sepharose-4B beads. Expression was monitored by blotting using an anti-GST antibody. Nucleolytic activity was measured by cleavage of plasmid DNA by EndoG variants. GST expressed and purified in parallel was used as a control. B, Stereo representation of an EndoG monomer in complex with double-stranded DNA (upper panel). The model has been obtained by superposition with the crystal structure of the Vvn–DNA complex,[43] in conjunction with limited energy minimisation. In order to analyse the putative protein DNA interface of an EndoG–DNA complex, the DNA from the Vvn–DNA complex has been extended in the lower panel. As can be seen from this model, Arg135 and Arg186 are in good positions to contact one strand of a double-stranded DNA-substrate, which is bound by EndoG *via* the minor groove.

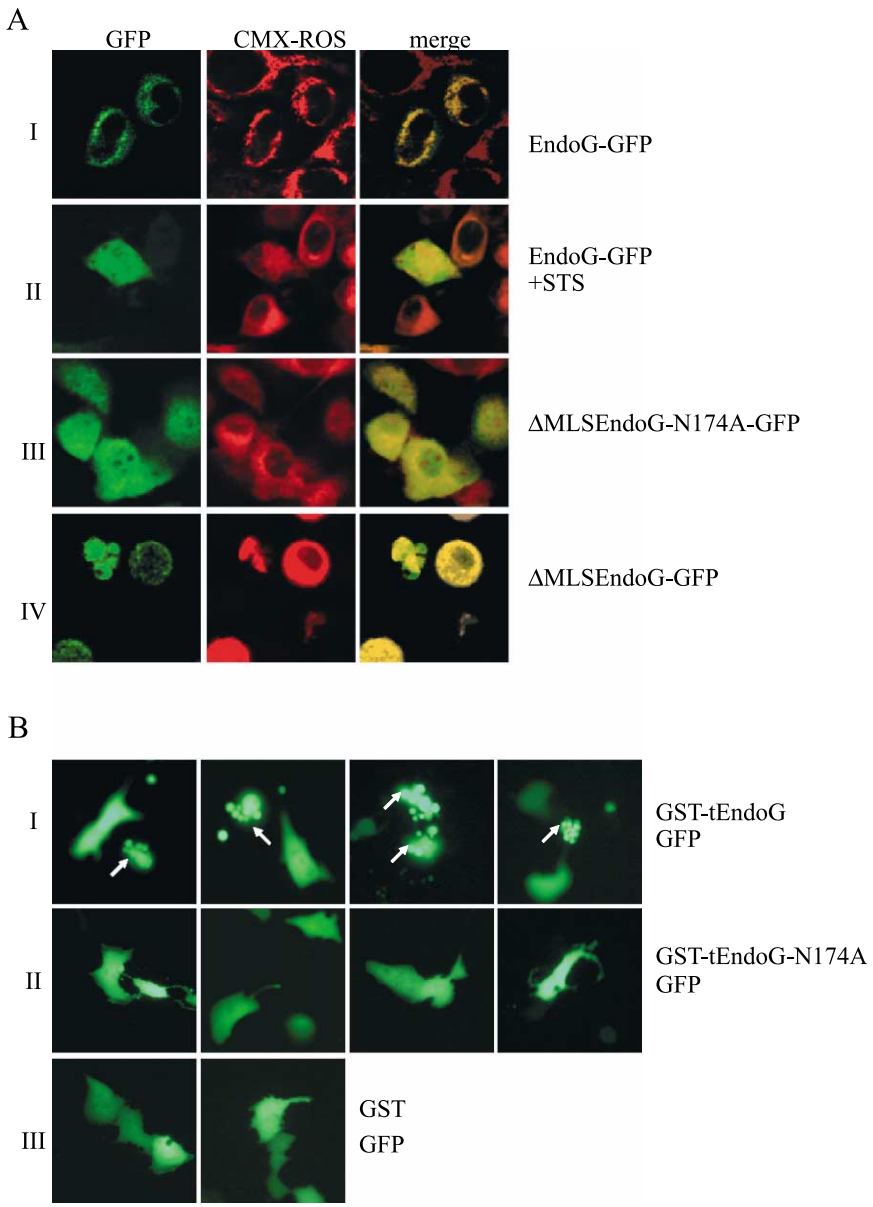

Figure 8. Transfection-mediated overexpression of extramitochondrial active tEndoG induces cell killing. A, Full-length EndoG-GFP-fusion protein transiently expressed in HeLa cells locates to the mitochondria (row I) and can be released into the cytosol and the nucleus upon treatment of the cells with staurosporine (+STS, 1 μM, 1 hour, row II). Transfection-mediated overexpression of extramitochondrial EndoG-GFP lacking the mitochondrial signal sequence (ΔMLSEndoG-GFP) induces cell killing in the case of an active enzyme variant (row IV), not however when an inactive variant (N174A) is used (row III). B, Co-transfection of CV1 cells with constructs encoding active or inactive GST-tEndoG variants and GFP reveal that active extramitochondrial EndoG induces cell death (row I), whereas an inactive EndoG variant (N174A, row II) or GST (row III) do not. Cells displaying apoptotic morphology are marked by arrows. Mitochondrial counterstaining was achieved using CMX-ROS (chloromethyl-X-rosamine).

nucleic acid binding (Figure 7B). Superposition of the DNA from the co-crystal structure of the DNA/RNA non-specific nuclease from *Vibrio vulnificus* (Vvn), strongly supports this hypothesis. Substitution of Arg135 by Ala or Lys and Arg186 by Ala or Lys leads to variants with 6–49% of wild-type activity, respectively, which is in the range expected for the alteration of a single basic amino acid residue among several others involved in substrate binding (Figure 7A and Table 1). Interestingly, in the model the arginine residues form contacts with only one strand of the double-stranded DNA substrate, suggesting that single and double-stranded nucleic acid substrates could be bound in a similar way.

Ectopic expression of active extramitochondrial EndoG leads to cell killing

A growing number of DNases as well as RNases have been used as devices in gene therapy in order to affect virus propagation or to kill tumour

cells.[33–37] Recently, a fusion protein of the caspase-activated DNase and GnRH was used to target cells derived from adenocarcinomas.[38] Using the results of our mutational analysis, we have tested the potential of ectopically expressed EndoG to induce cell killing. For this purpose, we have transfected HeLa and CV1 cells with constructs encoding full-length and truncated (lacking the mitochondrial leader sequence ΔMLS or tEndoG), active and inactive variants of EndoG (Figure 8).

In a first series of experiments, we have transfected HeLa cells with GFP-fusion constructs of full-length and truncated EndoG, and analysed the intracellular distribution of the expressed proteins by confocal laser scanning microscopy. Overexpression of full-length EndoG-GFP in HeLa cells, as expected, leads to the mitochondrial accumulation of the fusion protein as demonstrated by co-staining of mitochondria with CMX-ROS (Figure 8A, row I). Subsequent treatment of the cells with staurosporine, which induces apoptotic cell death, leads to the release of the protein into the cytosol and the nucleus of the transfected cells (Figure 8A, row II), demonstrating that mitochondrial uptake and release of a full-length EndoG-GFP fusion protein are not impaired by the GFP moiety. We have then investigated the localisation of truncated EndoG by transfecting GFP-fusion constructs of truncated EndoG lacking its mitochondrial signaling sequence (ΔMLS-EndoG-GFP). Truncated EndoG was found in the cytosol and the nucleus of transfected HeLa cells, similarly as full-length EndoG after induction of apoptosis by staurosporine (Figure 8A, rows III and IV).

Since it has been shown that the released, cytosolic form of EndoG is able to cause DNA fragmentation, we have, in a second series of experiments, investigated the potential of active and inactive truncated EndoG variants to induce cell killing. In these experiments, we have transfected HeLa and CV1 cells either with constructs coding for a fusion protein of active and inactive truncated EndoG and GFP (ΔMLSEndoG-GFP and ΔMLSEndoG-N174A-GFP) (Figure 8A rows III and IV), or co-transfected the cells with the constructs coding for GST-tEndoG and GST-tEndoG-N174A, together with GFP as a transfection marker (Figure 8B rows I and II). In all cases where active EndoG was used instead of the inactive variant N174A, the number of cells that displayed morphological signs indicative of apoptosis was significantly higher (Figure 8A rows III and IV; Figure 8B, rows I and II). In the case of HeLa cells transfected with constructs encoding active GST-tEndoG or inactive GST-tEndoG-N174A, respectively, we found 38% of the cells (437 cells counted) showing typical morphological signs of apoptosis in the case of active EndoG but only 11% (468 cells counted) in the case of the inactive variant EndoG-N174A, which is in accordance with the results obtained upon overexpression of active CPS-6/EndoG in *C. elegans*.[5] These results indicate that extramitochondrial EndoG, depending on its enzymatic activity, is able to trigger cell killing and open up the possibility to make use of this potential in anti-tumour therapy.

Conclusion

Here, we have performed a structural and functional characterisation of bovine EndoG. Homology modelling and biochemical data obtained for the wild-type enzyme and a variety of presumptive active-site mutants suggest that EndoG adopts a similar tertiary structure and follows a similar mechanism of action as the related *Serratia* nuclease. In addition, we have identified two arginine residues conserved strictly only in mammalian EndoG counterparts, which are likely to contribute to substrate binding. In line with our *in vitro* data, we show that ectopic expression of active extramitochondrial mature EndoG causes cell death in approximately 40% of the transfectants, whereas expression of an extramitochondrial inactive variant (N174A) or mitochondrial EndoG, does not. Our results demonstrate that active extramitochondrial EndoG by itself is able to trigger cell killing. The structural and functional similarity between EndoG and *Serratia* nuclease suggest that this may be caused by DNA as well as by RNA cleavage. Indeed, EndoG is not only able to cleave RNA *in vitro* but also *in vivo* (P.S., S.R.S. & G.M., unpublished results).

Materials and Methods

Plasmid construction

The cDNAs encoding the open reading frames of wild-type and mutant forms of truncated bovine EndoG (tEndoG, lacking the mitochondrial leader sequence (MLS, residues 1–48)) were inserted into an *Age*I and *Sal*I-digested modified pCI-vector (Promega), rendering plasmid pCI-GST-tEndoG, allowing expression of N-terminal GST-fusion proteins in transfected mammalian cells. GFP-fusion constructs of full length EndoG and truncated versions of EndoG, lacking the MLS, were generated by insertion of the cDNA in frame into the *Nhe*I and *Xho*I-digested vector pEGFP-N1 (BD-Clontech).

Cell culture and transfection

For the production of GST-tagged tEndoG in mammalian cells, HEK-293 cells (3–14 maxi-dishes/transfection) cultured at 37 °C in a humidified atmosphere of 5% CO_2 in DMEM with 10% (v/v) foetal calf serum, 100 units of penicillin and 100 μg/ml of streptomycin were transfected with 15 μg of an appropriate expression construct using Transfast™ transfection reagent (Promega) as described by the supplier's recommendations. GST-tEndoG was purified by GST-affinity chromatography as described by Korn *et al.*[39] using low-salt buffers.

To study the subcellular distribution of GFP-tagged EndoG variants, HeLa or CV1 cells, cultured in six-well

dishes under the same conditions as described above for HEK-293 cells, were transfected with 2 μg of each expression construct (1 μg + 1 μg when co-transfecting cells with two plasmids) using Polyfect transfection reagent (Qiagen) in the case of HeLa-cells and Transfast™ transfection reagent (Promega) in the case of CV1-cells, as described by the suppliers' recommendations. To induce apoptosis, cells were treated 18 hours post transfection with 1 μM (final concentration) staurosporine (Sigma-Aldrich) for one hour. To estimate the amount of apoptotic cells, 450 cells on average were counted per each transfection experiment in the case of HeLa cells.

Immunoblotting

EndoG and GST-tagged EndoG were detected after SDS-PAGE and electroblotting onto Hybond-ECL nitrocellulose membranes (Amersham Biosciences) using rabbit anti-EndoG antibody (α-EndoG, MobiTec) or a goat polyclonal anti-GST-antibody (α-GST, Amersham Biosciences), respectively. Horseradish peroxidase-conjugated anti-rabbit (Calbiochem) and anti-goat (Roche) antibodies were used as secondary antibodies in combination with enhanced chemiluminescence detection reagents (ECL) (Amersham Biosciences).

pH-dependence

To determine the pH-dependence of DNA cleavage by EndoG we have used a triple-buffer system (10 mM sodium acetate/10 mM Mes/20 mM Tris and 1 mM EDTA, adjusted with HCl or NaOH, respectively, from pH 4.5 to 10 in steps of 0.5 pH unit) that allows measuring a pH profile over a wide pH range without a change in buffer composition and at constant ionic strength, thus largely eliminating possible negative effects that frequently occur when switching between different buffer systems.[40] All cleavage reaction mixtures contained 25 ng/μl of plasmid DNA and 0.65 nM GST-tEndoG and were stopped after 15 minutes incubation at 37 °C by adding gel loading buffer. Cleavage products were analysed by electrophoresis on a TBE 0.8% agarose gel (100 mM Tris–HCl (pH 8.3), 100 mM borate, 2.5 mM EDTA) containing 0.05 μg/ml of ethidium bromide.

Salt and divalent metal ion cofactor dependence

Measurement of the salt-dependence of DNA cleavage by EndoG was performed in a buffer consisting of 10 mM sodium acetate/10 mM Mes/20 mM Tris adjusted with KOH to pH 6.0, 1 mM EDTA and 0, 25, 50, 75, 100, 125, 150, 175, 200, 250, 300 or 400 mM NaCl or KCl, respectively. Cleavage reactions were performed and analysed as described above.

To investigate the divalent metal ion preferences of DNA cleavage by EndoG we have used the same buffer as described above without monovalent cations but 2.5 mM final concentration of either Mg^{2+}, Mn^{2+}, Ca^{2+}, Ni^{2+}, Co^{2+}, Cu^{2+} or Zn^{2+}, respectively. In addition, we have investigated the divalent metal ion concentration dependence of EndoG-catalysed DNA cleavage for Mg^{2+}, Mn^{2+} and Co^{2+} over a range from 0 to 20 mM of each divalent metal ion cofactor.

Gel filtration

For an analysis of the quaternary structure of EndoG an aliquot of the GST-tEndoG fusion protein was incubated with thrombin overnight. Cleavage of the fusion protein was monitored by blotting using an anti-EndoG antibody. The cleaved fusion protein was then applied to a Superdex-75 HR 10/30 (bed dimensions: 10 mm × 300 mm) gel-filtration column equilibrated with 10 mM Hepes–KOH (pH 7.0), 100 mM KCl, 1 mM EDTA and 0.01% (v/v) Triton X-100 using a Merck-Hitachi HPLC-system. Approximately 15 μg of each variant was loaded onto the column in a volume of 100 μl and fractions of 1 ml were collected at a flow rate of 1 ml/minute. Aliquots (35 μl) of the fractions were incubated for one hour at 37 °C using 25 ng/μl (final concentration) of plasmid DNA (pBSK-VDEX). Cleavage products were analysed by agarose gel electrophoresis as described above.

Structural model

A model of the three-dimensional structure of bovine EndoG was generated based on the optimal alignment to the template structure of the *Serratia* nuclease (1g8t). The modelling and refinement of the EndoG structure was carried out as described by the "Frankenstein's monster" protocol.[41] Briefly, alternative models were generated by varying the parameters of the method and the quality of each model was assessed with VERIFY3D.[42] The best-scoring fragments were combined to produce a hybrid model. The procedure was reiterated until the VERIFY3D score could not be improved. The model of the EndoG dimer in complex with the DNA was obtained based on superposition with the crystal structure of the Vvn–DNA complex.[43] Contacts between the protein and the DNA were optimised by limited energy minimization.

Site-directed mutagenesis

Site-directed mutagenesis of EndoG was performed as described by Kirsch & Joly.[44] In brief, a first PCR was performed using a mutagenic primer and an appropriate reverse primer with pCI-GST-tEndoG as template, respectively, and Pfu DNA polymerase. Then, a second PCR was performed, using purified product from the first reaction as megaprimers for an inverse PCR following the instructions of the QuikChange protocol (Stratagene).

In vitro nuclease activity assays with wild-type EndoG and EndoG variants

Aliquots of GST-tagged Endo G variants were incubated in 20 mM Mes–KOH (pH 6.0), 1 mM EDTA, 6% (v/v) glycerol, 0.01% Triton-X-100, 1 mM DTT and 5 mM $MnCl_2$ or $MgCl_2$, respectively, for defined time intervals at 37 °C in the presence of 25 ng/μl of assay solution (10 nM final concentration) of plasmid DNA (pBSK-VDEX). Cleavage products were analysed by agarose gel electrophoresis as described above. Time-dependence of the disappearance of sc-plasmid DNA substrate catalysed by the nuclease variants compared to the wild-type enzyme was used to determine relative activities.

Microscopy

Fluorescence microscopy was performed with a Leica DMLB microscope equipped with a Leica HCX APO

L40X/0.80 W U-V-1 objective. Attached was a JVC TK-C1360 video-camera connected to a Pinnacle Systems Miro Video Capture Card to store digital images on a desktop computer. EGFP fluorescence was observed using a Leica Filterset I3. Mitochondrial counterstaining of living cells was achieved using the lipophilc dye CMX-ROS (chloromethyl-X-rosamine) also known as Mitotracker™ (Molecular Probes). Transfected cells were also examined with a Leica TCS4D confocal laser scanning microscope using a Leica HCX APO L40X/0.80 W U-V-1 objective. Excitation of GFP was achieved at 488 nm by a 75 mW Omnichrome argon/krypton laser. Emission was observed using a 580 nm beam splitter and a 510 nm longpass filter. Individual images were pseudocoloured. For life-cell imaging, transfected cells cultured in six-well dishes were transferred to and directly analysed under the microscopes 24–48 hours after transfection.

Acknowledgements

We are grateful to Dr Hanna Yuan for communicating results prior to publication and for allowing us to use the Vvn–DNA coordinates for structure comparison. We thank Ute Konradi for expert technical assistance and Dr Michael Knoblauch and Ingrid Schneider-Hüther for their help in confocal microscopy. This work has been supported by a grant from the Deutsche Forschungsgemeinschaft (Pi 122/16-1) and the Fonds der Chemischen Industrie. P.S. and S.R.S. are members of the Graduiertenkolleg "Biochemie von Nukleoproteinkomplexen". I.C.'s stay at Giessen was supported by the Deutsche Akademische Austauschdienst (International Quality Network "Biochemistry of Nucleic Acids"). J.M.B. acknowledges the support of the EMBO/HHMI Young Investigator Programme, Fellowship for Young Scientists from the Foundation for Polish Science and KBN (grant 3P04A01124).

References

1. Ruiz-Carrillo, A. & Renaud, J. (1987). Endonuclease G: a (dG)n X (dC)n-specific DNase from higher eukaryotes. *EMBO J.* **6**, 401–407.
2. Cote, J. & Ruiz-Carrillo, A. (1993). Primers for mitochondrial DNA replication generated by endonuclease G. *Science*, **261**, 765–769.
3. Huang, K. J., Zemelman, B. V. & Lehman, I. R. (2002). Endonuclease G, a candidate human enzyme for the initiation of genomic inversion in herpes simplex type 1 virus. *J. Biol. Chem.* **277**, 21071–21079.
4. Li, L. Y., Luo, X. & Wang, X. (2001). Endonuclease G is an apoptotic DNase when released from mitochondria. *Nature*, **412**, 95–99.
5. Parrish, J., Li, L., Klotz, K., Ledwich, D., Wang, X. & Xue, D. (2001). Mitochondrial endonuclease G is important for apoptosis in *C. elegans*. *Nature*, **412**, 90–94.
6. Zhang, J., Dong, M., Li, L., Fan, Y., Pathre, P., Dong, J. *et al.* (2003). Endonuclease G is required for early embryogenesis and normal apoptosis in mice. *Proc. Natl Acad. Sci. USA*, **100**, 15782–15787.
7. Rangarajan, E. S. & Shankar, V. (2001). Sugar nonspecific endonucleases. *FEMS Microbiol. Rev.* **25**, 583–613.
8. van Loo, G., Schotte, P., van Gurp, M., Demol, H., Hoorelbeke, B., Gevaert, K. *et al.* (2001). Endonuclease G.: a mitochondrial protein released in apoptosis and involved in caspase-independent DNA degradation. *Cell Death Differ.* **8**, 1136–1142.
9. Parrish, J. Z. & Xue, D. (2003). Functional genomic analysis of apoptotic DNA degradation in *C. elegans*. *Mol. Cell*, **11**, 987–996.
10. Miller, M. D., Tanner, J., Alpaugh, M., Benedik, M. J. & Krause, K. L. (1994). 2.1 A structure of *Serratia* endonuclease suggests a mechanism for binding to double-stranded DNA. *Nature Struct. Biol.* **1**, 461–468.
11. Kolmes, B., Franke, I., Friedhoff, P. & Pingoud, A. (1996). Analysis of the reaction mechanism of the non-specific endonuclease of *Serratia marcescens* using an artificial minimal substrate. *FEBS Letters*, **397**, 343–346.
12. Friedhoff, P., Kolmes, B., Gimadutdinow, O., Wende, W., Krause, K. L. & Pingoud, A. (1996). Analysis of the mechanism of the *Serratia* nuclease using site-directed mutagenesis. *Nucl. Acids Res.* **24**, 2632–2639.
13. Tiranti, V., Rossi, E., Ruiz-Carrillo, A., Rossi, G., Rocchi, M., DiDonato, S. *et al.* (1995). Chromosomal localization of mitochondrial transcription factor A (TCF6), single-stranded DNA-binding protein (SSBP), and endonuclease G (ENDOG), three human housekeeping genes involved in mitochondrial biogenesis. *Genomics*, **25**, 559–564.
14. Ohsato, T., Ishihara, N., Muta, T., Umeda, S., Ikeda, S., Mihara, K. *et al.* (2002). Mammalian mitochondrial endonuclease G. Digestion of R-loops and localization in intermembrane space. *Eur. J. Biochem.* **269**, 5765–5770.
15. Wang, X., Yang, C., Chai, J., Shi, Y. & Xue, D. (2002). Mechanisms of AIF-mediated apoptotic DNA degradation in *Caenorhabditis elegans*. *Science*, **298**, 1587–1592.
16. Widlak, P., Li, L. Y., Wang, X. & Garrard, W. T. (2001). Action of recombinant human apoptotic endonuclease G on naked DNA and chromatin substrates: cooperation with exonuclease and DNase I. *J. Biol. Chem.* **276**, 48404–48409.
17. Matsuyama, S., Llopis, J., Deveraux, Q. L., Tsien, R. Y. & Reed, J. C. (2000). Changes in intramitochondrial and cytosolic pH: early events that modulate caspase activation during apoptosis. *Nature Cell. Biol.* **2**, 318–325.
18. Cote, J., Renaud, J. & Ruiz-Carrillo, A. (1989). Recognition of (dG)n·(dC)n sequences by endonuclease G. Characterization of the calf thymus nuclease. *J. Biol. Chem.* **264**, 3301–3310.
19. Miller, M. D. & Krause, K. L. (1996). Identification of the *Serratia* endonuclease dimer: structural basis and implications for catalysis. *Protein Sci.* **5**, 24–33.
20. Franke, I., Meiss, G. & Pingoud, A. (1999). On the advantage of being a dimer, a case study using the dimeric *Serratia* nuclease and the monomeric nuclease from *Anabaena* sp. strain PCC 7120. *J. Biol. Chem.* **274**, 825–832.
21. Raaijmakers, H., Toro, I., Birkenbihl, R., Kemper, B. & Suck, D. (2001). Conformational flexibility in T4 endonuclease VII revealed by crystallography:

implications for substrate binding and cleavage. *J. Mol. Biol.* **308**, 311–323.
22. Kuhlmann, U. C., Moore, G. R., James, R., Kleanthous, C. & Hemmings, A. M. (1999). Structural parsimony in endonuclease active sites: should the number of homing endonuclease families be redefined? *FEBS Letters*, **463**, 1–2.
23. Cheng, Y. S., Hsia, K. C., Doudeva, L. G., Chak, K. F. & Yuan, H. S. (2002). The crystal structure of the nuclease domain of colicin E7 suggests a mechanism for binding to double-stranded DNA by the H-N-H endonucleases. *J. Mol. Biol.* **324**, 227–236.
24. Sui, M. J., Tsai, L. C., Hsia, K. C., Doudeva, L. G., Ku, W. Y., Han, G. W. & Yuan, H. S. (2002). Metal ions and phosphate binding in the H-N-H motif: crystal structures of the nuclease domain of ColE7/Im7 in complex with a phosphate ion and different divalent metal ions. *Protein Sci.* **11**, 2947–2957.
25. Flick, K. E., Jurica, M. S., Monnat, R. J., Jr & Stoddard, B. L. (1998). DNA binding and cleavage by the nuclear intron-encoded homing endonuclease I-PpoI. *Nature*, **394**, 96–101.
26. Galburt, E. A., Chevalier, B., Tang, W., Jurica, M. S., Flick, K. E., Monnat, R. J., Jr & Stoddard, B. L. (1999). A novel endonuclease mechanism directly visualized for I-PpoI. *Nature Struct. Biol.* **6**, 1096–1099.
27. Friedhoff, P., Franke, I., Meiss, G., Wende, W., Krause, K. L. & Pingoud, A. (1999). A similar active site for non-specific and specific endonucleases. *Nature Struct. Biol.* **6**, 112–113.
28. Walker, D. C., Georgiou, T., Pommer, A. J., Walker, D., Moore, G. R., Kleanthous, C. & James, R. (2002). Mutagenic scan of the H-N-H motif of colicin E9: implications for the mechanistic enzymology of colicins, homing enzymes and apoptotic endonucleases. *Nucl. Acids Res.* **30**, 3225–3234.
29. Scholz, S. R., Korn, C., Bujnicki, J. M., Gimadutdinow, O., Pingoud, A. & Meiss, G. (2003). Experimental evidence for a ββα-Me-finger nuclease motif to represent the active site of the caspase-activated DNase. *Biochemistry*, **42**, 9288–9294.
30. Shlyapnikov, S. V., Lunin, V. V., Perbandt, M., Polyakov, K. M., Lunin, V. Y., Levdikov, V. M. *et al.* (2000). Atomic structure of the *Serratia marcescens* endonuclease at 1.1 Å resolution and the enzyme reaction mechanism. *Acta Crystallog. sect. D*, **56**, 567–572.
31. Pommer, A. J., Cal, S., Keeble, A. H., Walker, D., Evans, S. J., Kuhlmann, U. C. *et al.* (2001). Mechanism and cleavage specificity of the H-N-H endonuclease colicin E9. *J. Mol. Biol.* **314**, 735–749.
32. Miller, M. D., Cai, J. & Krause, K. L. (1999). The active site of *Serratia* endonuclease contains a conserved magnesium–water cluster. *J. Mol. Biol.* **288**, 975–987.
33. Schumann, G., Cannon, K., Ma, W. P., Crouch, R. J. & Boeke, J. D. (1997). Antiretroviral effect of a gag-RNase HI fusion gene. *Gene Ther.* **4**, 593–599.
34. Schumann, G., Hermankova, M., Cannon, K., Mankowski, J. L. & Boeke, J. D. (2001). Therapeutic effect of a Gag-nuclease fusion protein against retroviral infection *in vivo*. *J. Virol.* **75**, 7030–7041.
35. Iordanov, M. S., Ryabinina, O. P., Wong, J., Dinh, T. H., Newton, D. L., Rybak, S. M. & Magun, B. E. (2000). Molecular determinants of apoptosis induced by the cytotoxic ribonuclease onconase: evidence for cytotoxic mechanisms different from inhibition of protein synthesis. *Cancer Res.* **60**, 1983–1994.
36. Saxena, S. K., Sirdeshmukh, R., Ardelt, W., Mikulski, S. M., Shogen, K. & Youle, R. J. (2002). Entry into cells and selective degradation of tRNAs by a cytotoxic member of the RNase A family. *J. Biol. Chem.* **277**, 15142–15146.
37. Haigis, M. C., Kurten, E. L. & Raines, R. T. (2003). Ribonuclease inhibitor as an intracellular sentry. *Nucl. Acids Res.* **31**, 1024–1032.
38. Ben-Yehudah, A., Aqeilan, R., Robashkevich, D. & Lorberboum-Galski, H. (2003). Using apoptosis for targeted cancer therapy by a new gonadotropin releasing hormone-DNA fragmentation factor 40 chimeric protein. *Clin. Cancer Res.* **9**, 1179–1190.
39. Korn, C., Scholz, S. R., Gimadutdinow, O., Pingoud, A. & Meiss, G. (2002). Involvement of conserved histidine, lysine and tyrosine residues in the mechanism of DNA cleavage by the caspase-3 activated DNase CAD. *Nucl. Acids Res.* **30**, 1325–1332.
40. Haq, I., O'Brien, R., Lagunavicius, A., Siksnys, V., Ladbury, J. E. & Specific, D. N. A. (2001). recognition by the type II restriction endonuclease MunI: the effect of pH. *Biochemistry*, **40**, 14960–14967.
41. Kosinski, J., Cymerman, I. A., Feder, M., Kurowski, M. A., Sasin, J. M. & Bujnicki, J. M. (2003). A "Frankenstein's monster" approach to comparative modeling: merging the finest fragments of fold-recognition models and iterative model refinement aided by 3D structure evaluation. *Proteins: Struct. Funct. Genet.* **53**, 369–379.
42. Eisenberg, D., Luthy, R. & Bowie, J. U. (1997). VERIFY3D: assessment of protein models with three-dimensional profiles. *Methods Enzymol.* **277**, 396–404.
43. Li, C. L., Hor, L. I., Chang, Z. F., Tsai, L. C., Yang, W. Z. & Yuan, H. S. (2003). DNA binding and cleavage by the periplasmic nuclease Vvn: a novel structure with a known active site. *EMBO J.* **22**, 4014–4025.
44. Kirsch, R. D. & Joly, E. (1998). An improved PCR-mutagenesis strategy for two-site mutagenesis or sequence swapping between related genes. *Nucl. Acids Res.* **26**, 1848–1850.

Edited by K. Morikawa

(Received 17 December 2003; received in revised form 11 February 2004; accepted 24 February 2004)